5. Métodos numéricos para os nanosistemas magnéticos

Full-Potential Linearized Augmented Plane Wave Method (FLAPW)

Stefan Blügel and Gustav Bihlmayer

Institute for Solid State Research, Jülich, Germany

Nos últimos dez anos os cálculos de primeiros princípios na base da teoria de funcional da densidade (DFT) na aproximação da densidade (de spin) local (LDA) ou de gradiente generalizado (GGA) formaram a ferramenta mais potente para descrição microscópica dos sistemas nanoestruturados. Os primeiros princípios se entendem como fixação dos parâmetros de teoria desde equações de mecânica quântica ou da DFT.

Os cálculos de Hartree-Fock tornam-se muito laboriosos com aumento de tamanho de sistema e necessitam um tempo crescente de processador para chegar á convergência. Uma alternativa muito simplificadora dentro da abordagem autoconsistente foi proposta por **W. Kohn** e **L. Sham** (1965), usando os resultados dos dois teoremas de **P. Hohenberg** e **W. Kohn** (1964).

O primeiro teorema HK diz que o estado fundamental do sistema de vários electrões está completamente definido (tanto energia como função de onda) pela densidade electrónica

$$n(\boldsymbol{r}) = |\psi(\boldsymbol{r})|^2$$

O segundo teorema HK estabelece que uso da densidade $n_0(\boldsymbol{r})$ na equação de Schroedinger minimiza a energia total do sistema.

Isso sugere a ideia principal do método de Kohn-Sham: passar de tratamento da função de onda no espaço de N vectores $\boldsymbol{r}_i$ ao tratamento da densidade $n(\boldsymbol{r})$, contribuida por todas partículas, mas que depende só num vector $\boldsymbol{r}$. Este metodo também se conhece como o de funcional da densidade electrónica (density functional theory, DFT).

Essencial da abordagem de Kohn-Sham

Energia e força totais

A DFT basea-se na representação da energia total do sistema dos átomos e electrões interactuantes como o funcional $E[\{\boldsymbol{R}\},\{\psi_i\}]$ das posições atómicas $\{\boldsymbol{R}\}$ e da densidade electrónica $n(\boldsymbol{r})$. A última está expressa através dos M orbitais de 1 partícula ocupados $\psi_i(\boldsymbol{r})$:

$$n(\boldsymbol{r}) = \sum_{i(oc)}^{M} |\psi_i(\boldsymbol{r})|^2 .$$

Se o funcional total $E[\{\boldsymbol{R}\},\{\psi_i\}]$ está minimizado com respeito aos graus de liberdade electrónicos $\{\psi_i\}$, recupera-se a superfície de Born-Oppenheimer:

$$\Phi[\{\boldsymbol{R}\}] = \min_{\{\psi_i\}} E[\{\boldsymbol{R}\},\{\psi_i\}],$$

a que define posições $\{\boldsymbol{R}\}$ dos átomos. A sua derivada define então a força:

$$\boldsymbol{F}^{\mu} = -\frac{\partial \Phi[\{\boldsymbol{R}\}]}{\partial \boldsymbol{R}_{\mu}} .$$

executada sobre o átomo μ e assim liga o problema electrónica a estrutura e dinâmicas cristalinas.

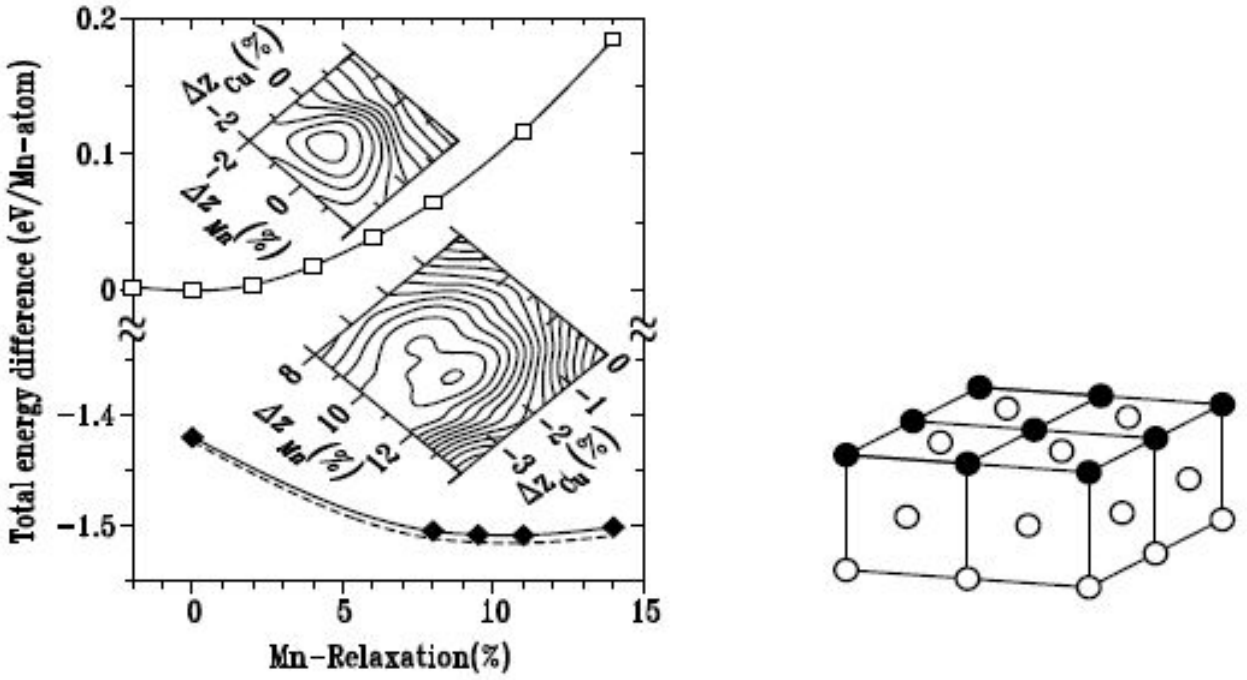

Figure 1. Example: structural optimization of Mn and Cu surface atoms in a Cu(100)c(2 × 2)Mn surface alloy. Right figure: Schematic representation of the substitutional surface alloy film of one monolayer thickness (• indicates the Mn atoms) grown as overlayer on a fcc (001) substrate (○). Left figure: Total energy per Mn atom vs. the buckling relaxation Δz_{Mn} of Mn in relative units with respect to the theoretical interlayer spacing of Cu, $d_{Cu} = 1.76$ Å. The open squares represent the nonmagnetic and the solid diamonds the ferromagnetic results. The solid lines (for Cu atoms fixed at the ideally terminated positions $\Delta z_{Cu} = 0$) and dashed line (the top Cu atom is always at its optimally relaxed position) are the fitting polynomials. The upper (lower) inset shows the contour plot of the nonmagnetic (ferromagnetic) total energy with respect to the buckling of Mn and Cu. The minimum, which determines the optimal structure is found in the inner circle. The contour interval is 1 meV. The energy of the nonmagnetic solution at 0% relaxation was chosen as the origin of the total energy scale (taken from Ref. 54).

A energia total apresenta-se como a soma dos termos consecutivos:

$$E[\{\boldsymbol{R}\},\{\psi_i\}] = E_{\mathrm{kin}}[\{\psi_i\}] + E_{\mathrm{H}}[\{\psi_i\}] + E_{\mathrm{xc}}[\{\psi_i\}] + E_{\mathrm{ext}}[\{\boldsymbol{R}\},\{\psi_i\}] + E_{\mathrm{ion}}[\{\boldsymbol{R}\}],$$

incluindo os termos de energia cinética dos electrões sem interacção, de Hartree (a energia clássica de Coulomb dos electrões) e de troca-correlação (as correlações devidas ao princípio de Pauli, ou "lacuna de troca", e à repulsão de Coulomb entre electrões e a contribuição à energia cinética dos electrões com interacção). No âmbito de LDA, o termo de troca-correlação apresenta-se como:

$$E_{\mathrm{xc}}[n] = \int d\boldsymbol{r}\, n(\boldsymbol{r})\varepsilon_{\mathrm{xc}}[n(\boldsymbol{r})].$$

Por fim os termos E_{ext} e E_{ion} descrevem respectivamente as interacções dos electrões com iões (potencial de tipo $1/r$) e entre os iões.

Equações de Kohn-Sham

Minimizando a energia total com respeito às funções de onda sujeitas à normalização:

$$\int d\boldsymbol{r}\, |\psi_i(\boldsymbol{r})|^2 = 1,$$

chegamos às equações de Kohn-Sham que definem o problema de auto-energias ε_i e auto-funções $\psi_i(\boldsymbol{r})$ de *uma* partícula:

$$\hat{H}[n]\psi_i[n] = \varepsilon_i[n]\psi_i[n],$$

com todas grandezas dependentes da densidade electrónica *n*. Conforme a estrutura da energia total, o Hamiltoniano também torna-se a soma dos termos correspondentes e o problema escreve-se como:

$$\left(\hat{T}_0 + \hat{V}_{ext} + \hat{V}_H + \hat{V}_{xc}\right)\psi_i(\boldsymbol{r}) = \varepsilon_i\psi_i(\boldsymbol{r}).$$

As formas particulares destes operadores no espaço directo são:

$$\hat{T}_0 = -\frac{\hbar^2}{2m}\nabla_{\boldsymbol{r}}{}^2, \quad \hat{V}_{ext}(\{\boldsymbol{R}\},\boldsymbol{r}) = \sum_\mu \frac{e^2 Z^\mu}{\left|\boldsymbol{r}-\boldsymbol{R}^\mu\right|},$$

$$\nabla_{\boldsymbol{r}}{}^2\hat{V}_H = 4\pi e^2 n(\boldsymbol{r}), \quad \hat{V}_{xc}(\boldsymbol{r}) = \frac{\delta}{\delta n(\boldsymbol{r})}\int d\boldsymbol{r} n(\boldsymbol{r})\varepsilon_{xc}(n(\boldsymbol{r})).$$

O potencial V_{ext} substitui-se pelo *pseudopotencial* V_{ps} na abordagem correspondente. Os termos de Hartree e de troca-correlação dependem da densidade electrónica local $n(\boldsymbol{r})$ a que no seu torno define-se pelas soluções $\psi_i(\boldsymbol{r})$ e assim define o problema de auto-consistência. Este problema resolve-se pelas iterações consecutivas até a densidade convergir a um limite com a precisão necessária.

No curso das iterações, as posições $\boldsymbol{R}^{\mu}$ dos átomos re-ajustam-se mantendo o mínimo da energia total do sistema, usando as dinâmicas moleculares com as forças $\boldsymbol{F}^{\mu}$.

As formas analiticas dos potenciais de troca-correlação incluem certas funções da densidade no âmbito de LDA e da densidade com as suas derivadas no âmbito de GGA.

O funcional $\varepsilon_{xc}[n(\boldsymbol{r})]$ inclui a derivada variacional e pode modelar-se como para gás electrónico uniforme (mas não livre!) de densidade n, relacionada ao parametro $r_s = (3/4\pi n)^{1/3} a_0$ (a_0 é o raio de Bohr). Por exemplo, **D. Ceperley** e **B. Alder** (1980) definiram este funcional em unidades de Hartree (1 H = $\hbar^2/ma_0^2 \approx$ 27.2 eV) como:

$$\varepsilon_{xc} = -\left(\frac{3}{2\pi}\right)^{2/3} \frac{1}{r_s} + A\ln r_s + \left(B - \frac{1}{3}A\right) + \frac{2}{3}Cr_s \ln r_s + \frac{1}{3}(2D - C)r_s,$$

$$A \approx 0.031, \quad B \approx -0.048, \quad C \approx 0.002, \quad D \approx -0.0116.$$

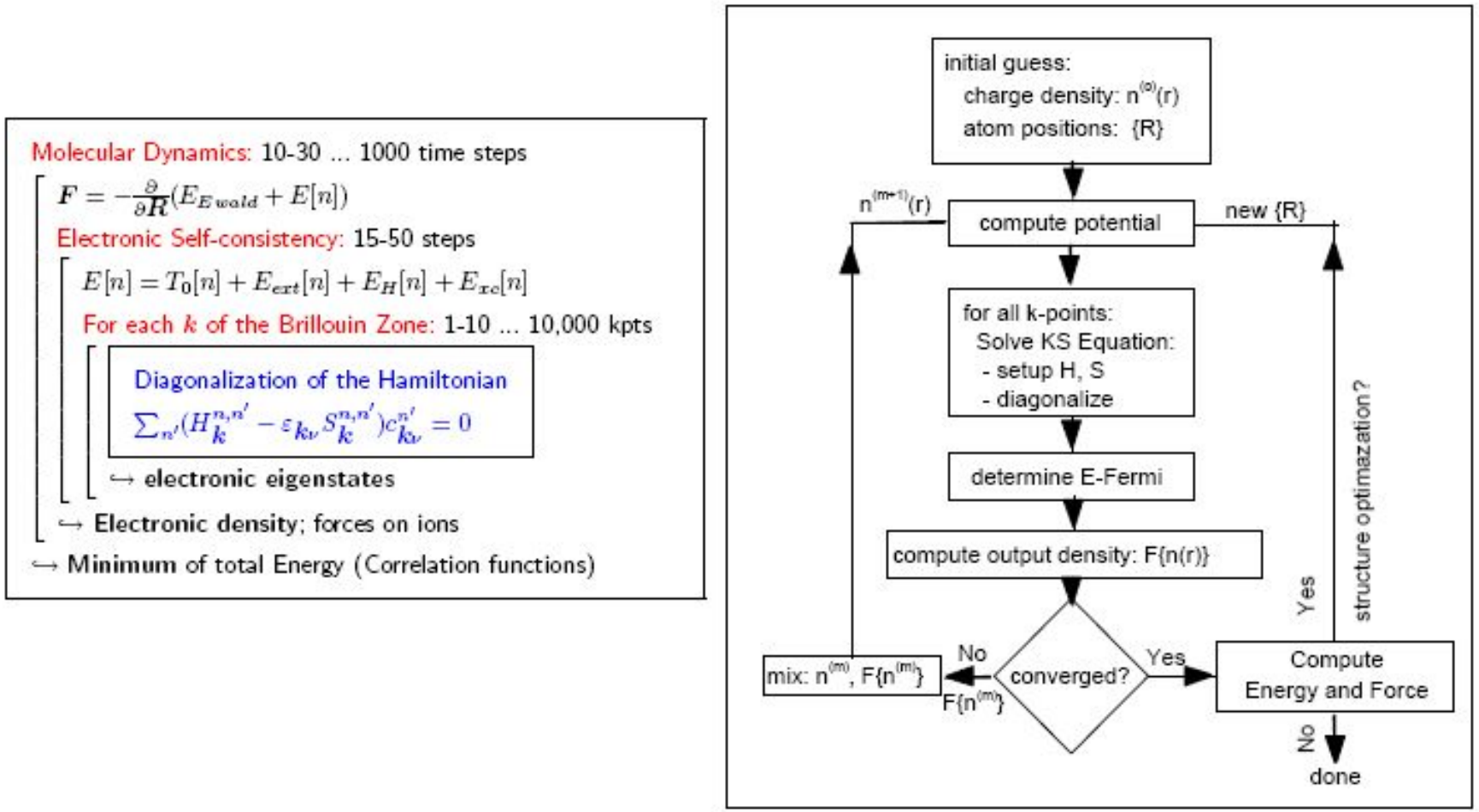

Figure 2. Right: Typical loop structure of a first-principles code based on density functional theory as applied to solid state materials. Left: Schematic flow-chart for self-consistent density functional calculations e.g. as realized by a FLAPW calculation.

Magnetism

If magnetism occurs, the ground state has a broken symmetry and the ground-state energy is described by functionals which depend on the vector-magnetization density $\mathbf{m}(\mathbf{r})$ as an additional field to the ordinary charge density $n(\mathbf{r})$, discussed so far. An additional term $\mu_B \underline{\boldsymbol{\sigma}} \cdot \mathbf{B}_{\mathrm{xc}}(\mathbf{r})$ appears in the Kohn-Sham equations Eq. (7), where $\mu_{\mathrm{B}} = \frac{e\hbar}{2mc}$ is the Bohr magneton, $\mathbf{B}_{\mathrm{xc}}$ is the magnetic xc-field an electron experiences, and $\underline{\boldsymbol{\sigma}}$ are the Pauli spinors. Thus, calculating magnetic systems, one works in a two-dimensional spin-space and the basis functions $\psi_{i\sigma}$ carry an additional spin label $\sigma = \pm 1$. The Hamiltonian is a 2×2 matrix in spin-space and is now hermitian and not symmetric. Complex magnetic structures lower frequently the symmetry of the problem and more states have to be calculated or a much larger fraction of the BZ (see Section 2.6) has to be sampled, respectively, pushing the computational effort to the limits of modern supercomputers. In case of collinear magnetism, e.g. ferro-, ferri-, or antiferromagnetism, $\underline{\boldsymbol{\sigma}} \cdot \mathbf{B}_{\mathrm{xc}}$ reduces to $\underline{\boldsymbol{\sigma}_z} \cdot B_{\mathrm{xc}}$, the Hamiltonian is diagonal in spin space, the magnetization density m_z is then given by spin-up and -down densities, $m_z(\mathbf{r}) = n_\uparrow(\mathbf{r}) - n_\downarrow(\mathbf{r})$, and the effort of a magnetic calculation is just twice that of a nonmagnetic one. In general, the magnetic moment $\mathbf{M} = \int d\mathbf{r}\, \mathbf{m}(\mathbf{r})$ is a vector quantity, and the search of the magnetic structure can be done dynamically bearing similarities to the dynamical structure optimization combining molecular dynamics and simulated annealing. Therefore, everything said in this chapter on structural optimization applies to both, the atomic and the magnetic structure. Throughout the paper, the spin label is dropped for convenience. More information on the treatment of magnetism can be found in the chapter "Non-collinear magnetism: exchange parameter and $\mathrm{T_C}$" by G. Bihlmayer.

The Eigenvalue Problem

In all-electron methods, eigenvalue problem Eq. (7) is solved for all occupied states i but typically subject to different boundary conditions. As shown schematically in Figure 3 we distinguish core electrons from valence electrons. The former have eigenenergies which are at least a couple of Rydbergs below the Fermi energy, the potential they experience is to an excellent approximation spherically symmetric and the wavefunctions have no overlap to neighboring atoms. The eigenvalue problem of these states is solved applying the boundary conditions of isolated atoms, which is numerically tackled by a shooting method. Valence electrons in a crystalline solid form electron bands and the eigenvalue problem is solved subject to the Bloch boundary conditions. The eigenstate is classified by the band index ν and a three-dimensional Bloch vector $\mathbf{k}$ within the first Brillouin zone, ($i \in \{\mathbf{k}\nu\}$). Some materials contain chemical elements with states (e.g. $5p$ states of $4f$ elements or W, p states of early transition metals) intermediate between band and core states and those are coined semicore states. These are high-lying and extended core states and particular care has to be taken on their treatment since their treatment as core states can cause significant errors in total energy, force and phonon calculations. According to the different treatment of the electrons, we decompose the charge density in the valence, semicore and core densities

$$n(\mathbf{r}) = n_{\mathrm{val}}(\mathbf{r}) + n_{\mathrm{sc}}(\mathbf{r}) + n_{\mathrm{core}}(r), \tag{12}$$

the latter being spherically symmetric. The charge densities are calculated according to Eq. (1). Wavefunctions and energies of core states give access to hyperfine quantities such as isomer shifts, hyperfine fields and electric field gradient as well as chemical shifts of core levels.

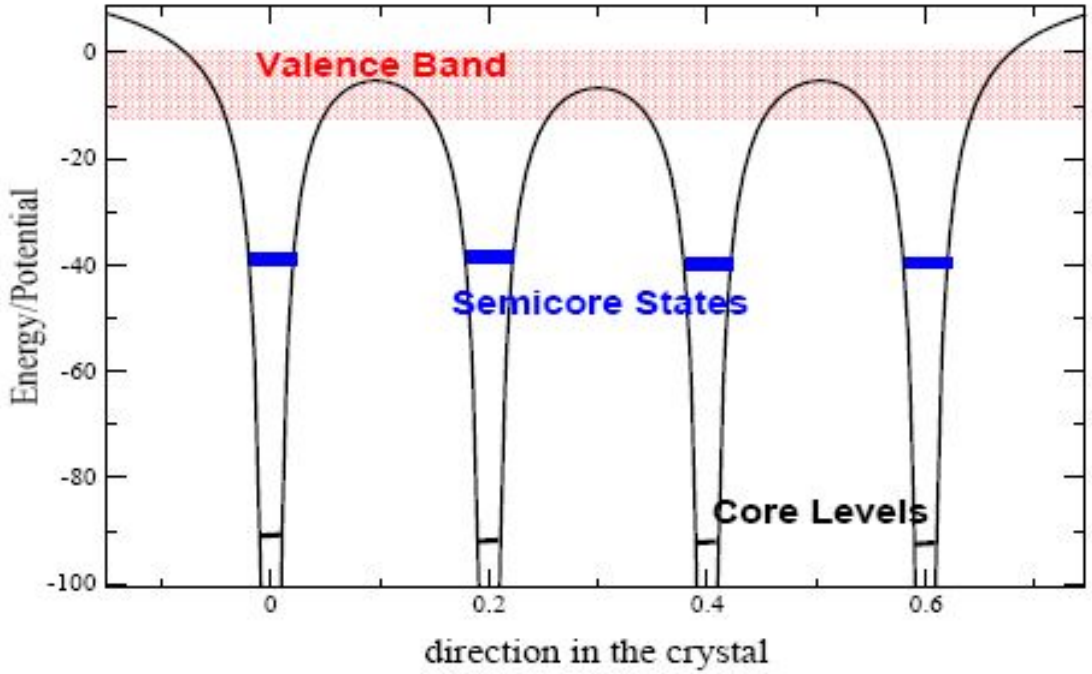

Figure 3. Schematic representation of the energy position of valence, semicore and core electrons in periodic potential.

There are many possible ways to solve the Kohn-Sham equations for valence electrons. Frequently, a variational method is chosen by which a wavefunction $\psi_{\mathbf{k}\nu}(\mathbf{r})$ of Bloch vector $\mathbf{k}$ and band index ν is sought as a linear combination of basis functions $\varphi_n(\mathbf{k}, \mathbf{r})$

$$\psi_{\mathbf{k}\nu}(\mathbf{r}) = \sum_{n=1}^{N} c_{\mathbf{k}\nu}^{n} \varphi_n(\mathbf{k}, \mathbf{r}) \tag{13}$$

satisfying the Bloch boundary conditions. $c_{\mathbf{k}\nu}^{n}$ are the expansion coefficients of the wavefunction (coefficient vector), and N is the number of basis functions taken into account. By this expansion, the eigenvalue problem

$$\hat{H}\psi_{\mathbf{k}\nu}(\mathbf{r}) = \varepsilon_{\mathbf{k}\nu}\psi_{\mathbf{k}\nu}(\mathbf{r}) \tag{14}$$

is translated into an algebraic eigenvalue problem of dimension N

$$(\mathrm{H}(\mathbf{k}) - \varepsilon_{\mathbf{k}\nu}\mathrm{S}(\mathbf{k}))\mathbf{c}_{\mathbf{k}\nu} = 0 \qquad \forall \mathbf{k} \in \mathrm{BZ} \tag{15}$$

for the coefficient vector $c^n_{\mathbf{k}\nu}$ corresponding to the eigenvalues $\varepsilon_{\mathbf{k}\nu}$. The Hamilton $H^{n,n'}(\mathbf{k})$ and overlap matrices $S^{n,n'}(\mathbf{k})$ are hermitian or real symmetric, depending on the point symmetry of the atomic structure. If the basis functions are orthonormal, i.e. $\langle\varphi_n|\varphi_{n'}\rangle = \delta^{n,n'}$, as for example in case of simple planewaves, then the overlap matrix S, defined as

$$S^{n,n'}(\mathbf{k}) = \int_\Omega \varphi^*_n(\mathbf{k},\mathbf{r})\varphi_{n'}(\mathbf{k},\mathbf{r})d^3r \tag{16}$$

becomes diagonal, $S^{n,n'}(\mathbf{k}) = \delta^{n,n'}$, and the generalized eigenvalue problem Eq. (15) becomes of standard type. Ω is the volume of the unit cell.

In general, the general eigenvalue problem is reduced to a standard one using the Cholesky decomposition. It can be shown (e.g. Stoer[61]), that any hermitian and positive definite matrix can be decomposed into a matrix product of a lower triangular matrix with only positive diagonal elements and its transposed. Clearly, the overlap matrix satisfies these conditions and can be written $\mathrm{S} = \mathrm{L}\mathrm{L}^{tr}$. Therefore, Eq. (15) becomes

$$\mathrm{H}\boldsymbol{c}_i = \varepsilon_i \mathrm{L}\mathrm{L}^{tr}\mathbf{c}_i, \tag{17}$$

multiplying from the left with L^{-1} and introducing a unit matrix we finally find

$$\mathrm{P}\mathbf{x}_i = \varepsilon_i \mathbf{x}_i, \tag{18}$$

after we have P defined as $\mathrm{P} = \mathrm{L}^{-1}\mathrm{H}(\mathrm{L}^{-1})^{tr}$ and $\mathbf{x}_i = \mathrm{L}^{tr}\mathbf{c}_i$. Thus, the generalized eigenvalue problem has been reduced to a simple one. The eigenvectors $\mathbf{c}_i$ can be obtained by the back-transformation, $\mathbf{c}_i = (\mathrm{L}^{tr})^{-1}\mathbf{x}_i$.

The choice of the most efficient numerical algorithm to solve Eq. (15) depends on the number of basis functions N and the number M of states ν taken into account. If $M/N > \sim 0.1$, direct numerical diagonalization schemes are employed, for example parallelized eigenvalue solvers taken from the ScaLAPACK library package. If $M/N <\sim 0.1$ or if N is too large to fit the eigenvalue problem into the memory of a computer the eigenvalue problem is solved iteratively. Any iterative solution of an eigenvalue problem can be divided into two parts: (i) the determination of the iterative improvement of the state vector $c_{\mathbf{k}\nu}^{n,[m]}$ at iteration step m by multiplying the Hamiltonian with the state vector to obtain the update $c_{\mathbf{k}\nu}^{n,[m+1]}$:

$$c_{\mathbf{k}\nu}^{n,[m+1]} = \sum_{n'} H^{n,n'}(\mathbf{k}) c_{\mathbf{k}\nu}^{n',[m]}, \tag{19}$$

and (ii) the orthonormalization of the wavefunctions

$$\sum_{n} c_{\mathbf{k}\nu}^{n,[m+1]} c_{\mathbf{k}\nu'}^{n,[m+1]} = \delta_{\nu,\nu'}. \tag{20}$$

(iii) Frequently, each iteration step is accompanied by a direct sub-space diagonalization of a dimension proportional to M, on which Hamiltonian $\hat{H}$ is projected. If the multiplication of $\mathrm{H} \cdot \mathbf{c}$ can be made fast by expressing the Hamiltonian in terms of dyadic products or convolutions as in norm-conserving or ultra-soft pseudo-potentials minimizing thereby the number of multiplications, iterative methods become particular beneficial.

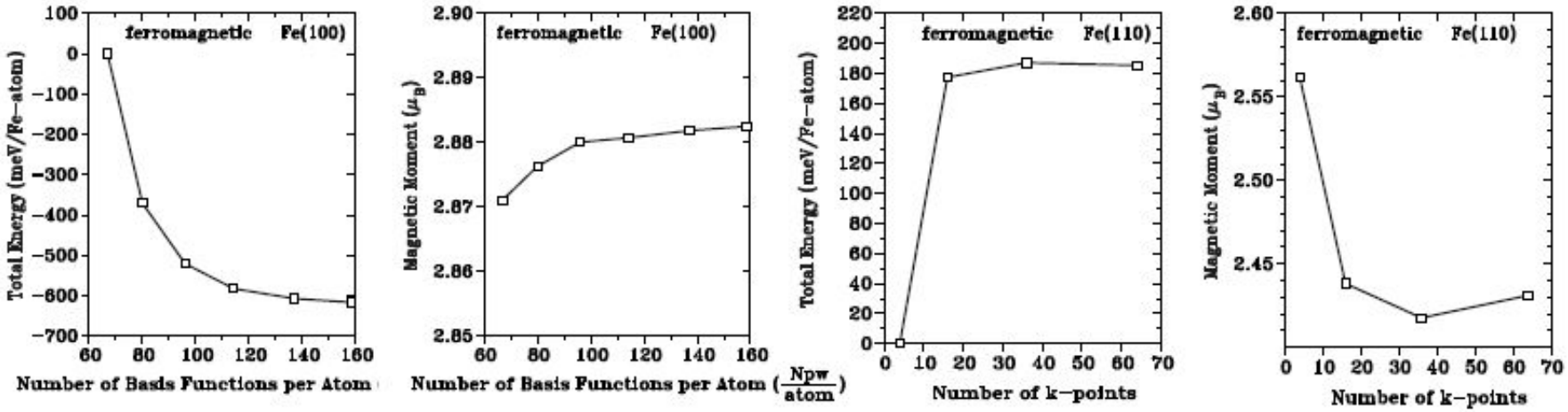

Figure 4. Test of convergence carried out by the FLAPW method of (absolute) total energy and magnetic moment as function (i) of the number of the LAPW basis functions (see two left figures) for a 7 layer Fe(100) film and (ii) number of special **k**-points in the IBZ (see two right figures) for an 11 layer Fe(110) film. The calculations of (i) were carried out for the rkm-parameters $rkm = 7.5, 8.0, 8.5, 9.0, 9.5, 10.0$ corresponding to $N = 67, 80, 96, 114, 137, 158$ basis functions.

The FLAPW Method

The full-potential LAPW method (FLAPW)[24, 12] combines the choice of the LAPW basis set with the treatment of the full-potential and charge density without any shape-approximations in the interstitial region and inside the muffin-tins. This generalization is achieved by relaxing the constant interstitial potential V_I^0 and the spherical muffin-tin approximation $V_{MT}^0(r)$ due to the inclusion of a warped interstitial $\sum V_I^{\mathbf{G}} e^{i\mathbf{G}\mathbf{r}}$ and the non-spherical terms inside the muffin-tin spheres:

$$V(\mathbf{r}) = \begin{cases} \sum_{\mathbf{G}} V_I^{\mathbf{G}} e^{i\mathbf{G}\mathbf{r}} & \text{interstitial region} \\ \sum_{L} V_{MT}^{L}(r) Y_L(\hat{\mathbf{r}}) & \text{muffin-tin .} \end{cases} \tag{54}$$

This method became possible with the development of a technique for obtaining the Coulomb potential for a general periodic charge density without shape-approximations and with the inclusion of the Hamiltonian matrix elements due to the warped interstitial and non-spherical terms of the potential. The charge density n is represented analogously to Eq. (54), just exchanging V by n. Details of the solution of the Poisson equation for an arbitrarily shaped periodic potential are described in Section 4.6.

Construction of the HamiltonianMatrix

The FLAPW Hamiltonian and overlap matrices consist of two contributions from the two regions into which space is divided.

$$\mathrm{H} = \mathrm{H}_I + \mathrm{H}_{MT} \qquad \text{and} \qquad \mathrm{S} = \mathrm{S}_I + \mathrm{S}_{MT} \tag{55}$$

Both contributions have to be computed separately.

Contribution of the Muffin-Tins

Writing the product of the radial functions u with the spherical harmonics as $\phi_L = u_l Y_L$, the contribution of the muffin-tin to the Hamiltonian matrix and the overlap matrix is given by:

$$H_{MT}^{\mathbf{G}'\mathbf{G}}(\mathbf{k}) = \sum_{\mu} \int_{MT^{\mu}} \left(\sum_{L'} a_{L'}^{\mu\mathbf{G}'}(\mathbf{k}) \phi_{L'}^{\alpha}(\mathbf{r}) + b_{L'}^{\mu\mathbf{G}'}(\mathbf{k}) \dot{\phi}_{L'}^{\alpha}(\mathbf{r}) \right)^{*} \hat{H}_{MT^{\alpha}} \left(\sum_{L} a_{L}^{\mu\mathbf{G}}(\mathbf{k}) \phi_{L}^{\alpha}(\mathbf{r}) + b_{L}^{\mu\mathbf{G}}(\mathbf{k}) \dot{\phi}_{L}^{\alpha}(\mathbf{r}) \right) d^3r \ . \tag{56}$$

(The overlap matrix $S_{MT}^{\mathbf{G}'\mathbf{G}}(\mathbf{k})$ is obtained by replacing $\hat{H}_{MT^\alpha}$ by 1.) It is distinguished between the atom index μ and the atom type index $\alpha(\mu)$. In most applications they are symmetry equivalent atoms in the unit cell, i.e. some atoms can be mapped onto each other by space group operations. Clearly, these atoms must possess the same physical properties, e.g. the potential has to be equal. As a consequence, the Hamiltonian and the basis functions $\varphi_L^\alpha(\mathbf{r})$ do not differ among the atoms of the same type. This fact is exploited in that the muffin-tin potential of an atom type is only stored once for the representative atom, and the matrices in Eq. (58) are also calculated for the representative only. $\hat{H}_{MT^\alpha}$ is the scalar relativistic Hamiltonian operator. It can be split up into two parts, the spherical Hamiltonian $\hat{H}_{sp}$ (cf. Eq. (40)) and the nonspherical contributions to the potential V_{ns}.

$$\hat{H}_{MT^\alpha} = \hat{H}_{sp}^\alpha + V_{ns}^\alpha \tag{57}$$

The above integrations contain the following type of matrix elements:

$$t_{L'L}^{\alpha\phi\phi} = \int_{MT^\alpha} \phi_{L'}^\alpha(\mathbf{r}) \hat{H}_{MT^\alpha} \phi_L^\alpha(\mathbf{r}) d^3r \ . \tag{58}$$

These matrix elements do not depend on the $A_L^{\mu\mathbf{G}}(\mathbf{k})$ and $B_L^{\mu\mathbf{G}}(\mathbf{k})$ coefficients. Thus, they are independent of the Bloch vector and need to be calculated only once per iteration. The functions ϕ_L^α and $\dot{\phi}_L^\alpha$ have been constructed to diagonalize the spherical part $\hat{H}_{sp}^\alpha$ of the muffin-tin Hamiltonian $\hat{H}_{MT^\alpha}$:

$$\hat{H}_{sp}^\alpha \phi_L^\alpha = E_l \phi_L^\alpha \quad \text{and} \quad \hat{H}_{sp}^\alpha \dot{\phi^\alpha}_L + = E_l \dot{\phi}_L^\alpha + \phi_L^\alpha. \tag{59}$$

Multiplying these equations with $\phi^{\alpha}_{L'}(\mathbf{r})$ and $\dot{\phi}^{\alpha}_{L'}(\mathbf{r})$ respectively and integrating over the muffin-tins gives

$$\langle\phi^{\alpha}_{L'}|\hat{H}^{\alpha}_{sp}\phi^{\alpha}_{L}\rangle_{MT^{\alpha}} = \delta_{ll'}\delta_{mm'}E_l \quad ; \quad \langle\phi^{\alpha}_{L'}|\hat{H}^{\alpha}_{sp}\dot{\phi}^{\alpha}_{L}\rangle_{MT^{\alpha}} = \delta_{ll'}\delta_{mm'}$$
$$\langle\dot{\phi}^{\alpha}_{L'}|\hat{H}^{\alpha}_{sp}\phi^{\alpha}_{L}\rangle_{MT^{\alpha}} = 0 \quad ; \quad \langle\dot{\phi}^{\alpha}_{L'}|\hat{H}^{\alpha}_{sp}\dot{\phi}^{\alpha}_{L}\rangle_{MT^{\alpha}} = \delta_{ll'}\delta_{mm'}E_l\langle\dot{u}^{\alpha}_{l}|\dot{u}^{\alpha}_{l}\rangle_{MT^{\alpha}} \ , \quad (60)$$

where the normalization condition for u^{α}_{l} has been used. So, only the expectation values of the nonspherical part of the potential are left to be determined. Since the potential is also expanded into a product of radial functions and spherical harmonics,

$$V^{\alpha}(\mathbf{r}) = \sum_{L''} V^{\alpha}_{L''}(r)Y_{L''}(\hat{\mathbf{r}}), \quad (61)$$

the corresponding integrals consist of a product of radial integrals and angular integrals over three spherical harmonics, the so-called Gaunt coefficients:

$$t^{\alpha\phi\phi}_{L'L} = \sum_{l''} I^{\alpha uu}_{l'll''}G^{m'mm''}_{l'll''} + \delta_{ll'}\delta_{mm'}E_l \quad (62)$$

with

$$G^{mm'm''}_{ll'l''} = \int Y^{*}_{lm}Y_{l'm'}Y_{l''m''}d\Omega \quad \text{and} \quad I^{\alpha uu}_{l'll''} = \int u^{\alpha}_{l'}(r)u^{\alpha}_{l}(r)V^{\alpha}_{l''}(r)r^2dr \quad (63)$$

as well as similar expressions for $I^{\alpha u\dot{u}}_{l'll''}$ and others. The I matrices contain the radial integrals. Finally, the Hamiltonian and overlap matrix elements become

$$H_{MT}^{\mathbf{G}'\mathbf{G}}(\mathbf{k}) = \sum_{\mu}\sum_{L'L}(a_{L'}^{\mu\mathbf{G}'}(\mathbf{k}))^* t_{L'L}^{\alpha\phi\phi} a_{L}^{\mu\mathbf{G}}(\mathbf{k}) + (b_{L'}^{\mu\mathbf{G}'}(\mathbf{k}))^* t_{L'L}^{\alpha\dot{\phi}\dot{\phi}} b_{L}^{\mu\mathbf{G}}(\mathbf{k})$$
$$+(a_{L'}^{\mu\mathbf{G}'}(\mathbf{k}))^* t_{L'L}^{\alpha\phi\dot{\phi}} b_{L}^{\mu\mathbf{G}}(\mathbf{k}) + (b_{L'}^{\mu\mathbf{G}'}(\mathbf{k}))^* t_{L'L}^{\alpha\dot{\phi}\phi} a_{l}^{\mu\mathbf{G}}(\mathbf{k}) \ , \qquad (64)$$

$$S_{MT}^{\mathbf{G}'\mathbf{G}}(\mathbf{k}) = \sum_{\mu}\sum_{L}(a_{L}^{\mu\mathbf{G}'}(\mathbf{k}))^* a_{L}^{\mu\mathbf{G}}(\mathbf{k}) + (b_{L}^{\mu\mathbf{G}'}(\mathbf{k}))^* b_{L}^{\mu\mathbf{G}}(\mathbf{k}) \langle \dot{u}_l^{\alpha} | \dot{u}_l^{\alpha} \rangle_{MT^{\mu}} \ . \qquad (65)$$

The Interstitial Contribution

The interstitial contributions to the Hamiltonian and overlap matrix have the following form:

$$H_I^{\mathbf{G}\mathbf{G}'}(\mathbf{k}) = \frac{1}{\Omega}\int_I e^{-i(\mathbf{G}+\mathbf{k})\mathbf{r}} \left(-\frac{\hbar^2}{2m}\triangle + V(\mathbf{r})\right) e^{i(\mathbf{G}'+\mathbf{k})\mathbf{r}} d^3r \ , \qquad (66)$$

$$S_I^{\mathbf{G}\mathbf{G}'} = \frac{1}{\Omega}\int_I e^{-i(\mathbf{G}+\mathbf{k})\mathbf{r}} e^{i(\mathbf{G}'+\mathbf{k})\mathbf{r}} d^3r \ . \qquad (67)$$

The potential is also expanded into planewaves in the interstitial region:

$$V(\mathbf{r}) = \sum_{\mathbf{G}'} V_{\mathbf{G}'} e^{-i\mathbf{G}\mathbf{r}} \ . \qquad (68)$$

Without the existence of the muffin-tin spheres the integration would stretch over the entire unit cell and the integration would become rather simple. The kinetic energy is diagonal in momentum space and the potential is local, diagonal is real space and of convolution form in momentum space.

$$H_I^{\mathbf{G}\mathbf{G}'}(\mathbf{k}) = \frac{\hbar^2}{2m}|\mathbf{G}+\mathbf{k}|^2\delta_{\mathbf{G}\mathbf{G}'} + V_{(\mathbf{G}-\mathbf{G}')} \ ,$$

$$S_I^{\mathbf{G}\mathbf{G}'} = \delta_{\mathbf{G}\mathbf{G}'} \ .$$

However, these matrix elements are not as straightforward to calculate as they appear at first glance, because of the complicated structure of the interstitial region. The integrations have to be performed only in between the muffin-tins. Therefore, a step function $\Theta(\mathbf{r})$ has to be introduced, that cuts out the muffin-tins:

$$\Theta(\mathbf{r}) = \begin{cases} 1 \text{ interstitial region} \\ 0 \text{ muffin-tins} \ . \end{cases} \tag{69}$$

Using the step function the matrix elements can be written as:

$$H_I^{\mathbf{G}\mathbf{G}'}(\mathbf{k}) = \frac{1}{\Omega}\int_{cell} e^{-i(\mathbf{G}-\mathbf{G}')\mathbf{r}} V(\mathbf{r})\Theta(\mathbf{r})d^3r + \frac{1}{2}(\mathbf{G}'+\mathbf{k})^2\frac{1}{\Omega}\int_{cell} e^{-i(\mathbf{G}-\mathbf{G}')\mathbf{r}}\Theta(\mathbf{r})d^3r \ , \tag{70}$$

$$S_I^{\mathbf{G}\mathbf{G}'} = \frac{1}{\Omega}\int_{cell} e^{-i(\mathbf{G}-\mathbf{G}')\mathbf{r}}\Theta(\mathbf{r})d^3r \ . \tag{71}$$

In momentum space Eq. (70) becomes:

$$H_I^{\mathbf{G}\mathbf{G}'}(\mathbf{k}) = (V\Theta)_{(\mathbf{G}-\mathbf{G}')} + \frac{\hbar^2}{2m}(\mathbf{G}'+\mathbf{k})^2\Theta_{(\mathbf{G}-\mathbf{G}')} \ , \tag{72}$$

$$S_I^{\mathbf{G}\mathbf{G}'} = \Theta_{(\mathbf{G}-\mathbf{G}')} \ , \tag{73}$$

where $\Theta_{\mathbf{G}}$ and $(V\Theta)_{\mathbf{G}}$ are the Fourier coefficients of $\Theta(\mathbf{r})$ and $V(\mathbf{r})\Theta(\mathbf{r})$ respectively. Apparently these coefficients are needed up to a cutoff of $2G_{\max}$. The step function can be Fourier transformed analytically:

$$\Theta_{\mathbf{G}} = \delta_{\mathbf{G},0} - \sum_{\mu} e^{-i\mathbf{G}\boldsymbol{\tau}^{\mu}} \quad \frac{4\pi (R_{MT}^{\alpha})^3}{\Omega} \frac{j_1(GR_{MT}^{\alpha})}{GR_{MT}^{\alpha}} ,$$

where $\boldsymbol{\tau}^{\mu}$ indicates the position of atom μ. The Fourier transform of the product of $V(\mathbf{r})$ and $\Theta(\mathbf{r})$ is given by a convolution in momentum space:

$$(V\Theta)_{\mathbf{G}} = \sum_{\mathbf{G}'} V_{\mathbf{G}'} \Theta_{(\mathbf{G}-\mathbf{G}')} \cdot$$

This convolution depends on both, $\mathbf{G}$ and $\mathbf{G}'$, therefore the numerical effort increases like $(G_{\max})^6$. However, $(V\Theta)_{\mathbf{G}}$ can be determined more efficiently, using Fast Fourier Transform (FFT). In Figure 10 it is shown schematically how $(V\Theta)_{\mathbf{G}}$ can be obtained using FFT. Using this scheme the numerical effort increases like $(G_{\max})^3 \ln(G_{\max})^3$ with $G_{\max}$.

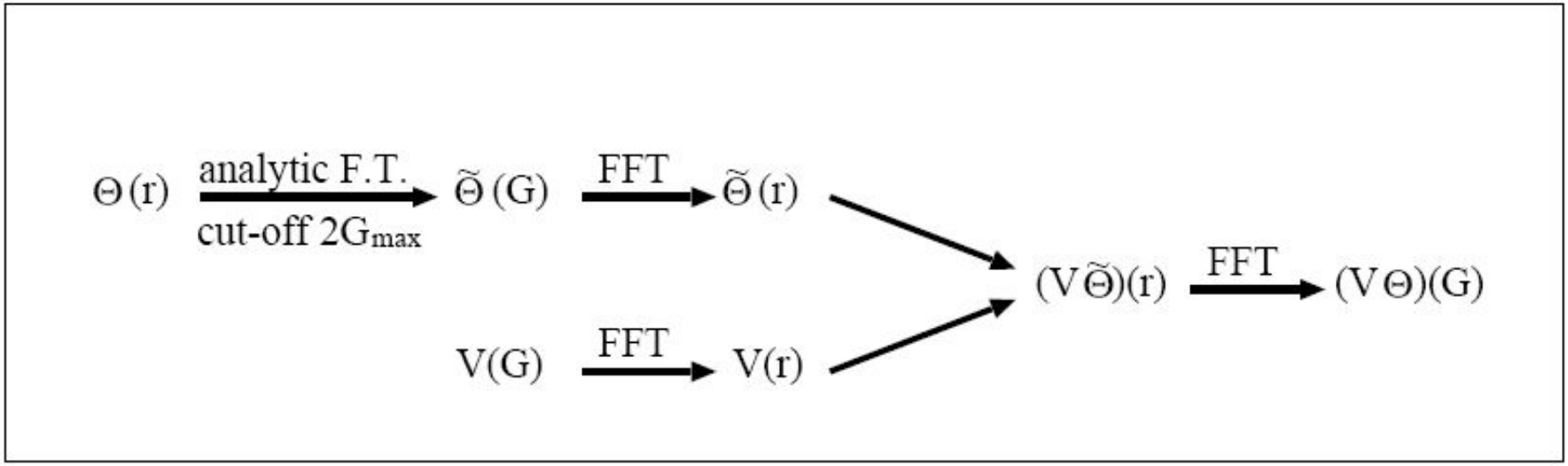

Figure 10. Schematic representation of the calculation of $(V\Theta)_{\mathbf{G}}$. First $\Theta(\mathbf{r})$ is Fourier transformed analytically with a cutoff of $2G_{\max}$ yielding $\tilde{\Theta}_{\mathbf{G}}$. Then $\tilde{\Theta}_{\mathbf{G}}$ and $V_{\mathbf{G}}$ are fast Fourier transformed and multiplied on a real space mesh. Finally, the result $(V\tilde{\Theta})(\mathbf{r})$ is back-transformed to momentum space.

The FLAPW Method for Specialized Geometries

The Film Geometry for Surfaces and Thin Films

Today, the physics of surfaces and films is an field of major interest and investigation. However, surfaces are difficult to treat, because they break the translational symmetry, i.e. there is only the 2-dimensional symmetry parallel to the surface left to be used to reduce the problem, and a semi-infinite problem is left perpendicular to the surface. In our approach surfaces are approximated by thin films, typically 10–15 atomic layers thick. Obviously, this approximation, which is called the thin-slab approximation, can only yield good results if the interaction between the two surfaces of the film is week enough, so that each of them shows the properties of the surfaces of an ideal semi-infinite crystal. In the case of film calculations space is divided into three distinct regions, the muffin-tins, the interstitial and the vacuum region (cf. Figure 12). The interstitial region now stretches from $-D/2$ to $D/2$ in z-direction, which is defined to be the direction perpendicular to the film. The representation of the wavefunctions inside the muffin-tin spheres remains exactly the same as in the bulk case. Since the periodicity along the z-direction is lost, the unit cell extends principally from $-\infty$ to ∞ in z-direction. Still the wavefunctions can be expanded in terms of planewaves. However, the wavevectors perpendicular to the film are not defined in terms of D, but in terms of $\tilde{D}$, which is chosen larger than D to gain greater variational freedom. Therefore, the planewaves have the form

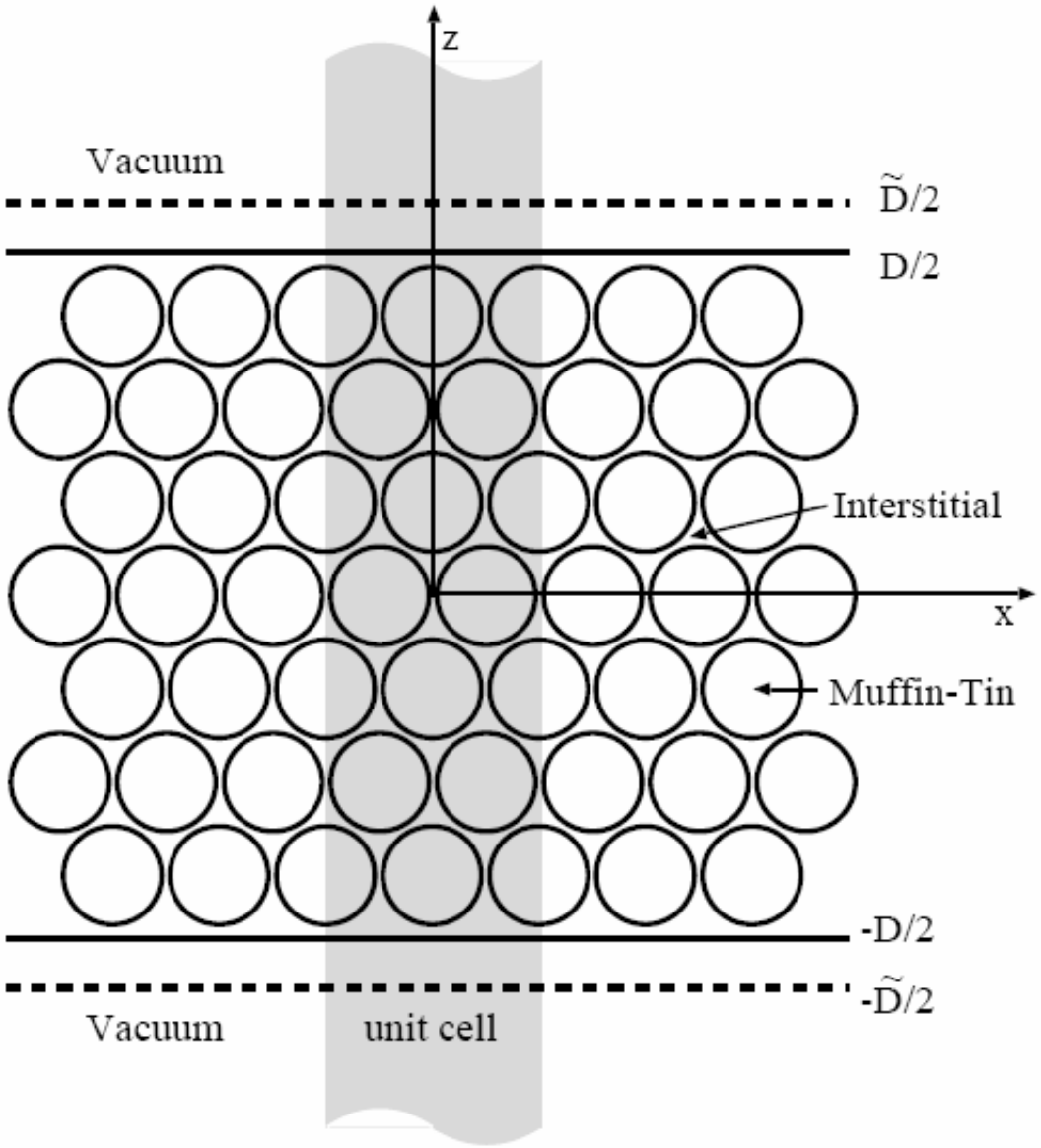

Figure 12. The unit cell in film calculations contain two semi-infinite vacuum regions.

$$\varphi_{\mathbf{G}_\parallel G_\perp}(\mathbf{k}_\parallel, \mathbf{r}) = e^{i(\mathbf{G}_\parallel + \mathbf{k}_\parallel)\mathbf{r}_\parallel}\ e^{iG_\perp z} \qquad \text{with} \qquad G_\perp = \frac{2\pi n}{\tilde{D}}, \tag{124}$$

where $\mathbf{G}_\parallel$ and $\mathbf{k}_\parallel$ are the 2-dimensional wave- and Bloch vectors, $\mathbf{r}_\parallel$ is the parallel component of $\mathbf{r}$ and $G_\perp$ is the wavevector perpendicular to the film. The basis functions in the vacuum region are constructed in the same spirit as the functions in the muffin-tins. They consist of planewaves parallel to the film, and a z-dependent function $u_{\mathbf{G}_\parallel}(\mathbf{k}_\parallel, z)$, which solves the corresponding one-dimensional Schrödinger equation Eq. (125), plus its energy derivative $\dot{u}_{\mathbf{G}_\parallel}(\mathbf{k}_\parallel, z)$:

$$\left\{ -\frac{\hbar^2}{2m}\frac{\partial^2}{\partial z^2} + V_0(z) - E_{vac} + \frac{\hbar^2}{2m}(\mathbf{G}_\parallel + \mathbf{k}_\parallel)^2 \right\} u_{\mathbf{G}_\parallel}(\mathbf{k}_\parallel, z) = 0\ . \tag{125}$$

E_{vac} is the vacuum energy parameter and $V_0(z)$ is the planar averaged part of the vacuum potential. As in the case of $\dot{u}_l$ in the muffin-tins, the function $\dot{u}_{\mathbf{G}_\parallel}(\mathbf{k}_\parallel, z)$ is calculated from a Schrödinger-like equation, which can be obtained by deriving Eq. (125) with respect to the energy:

$$\left\{ -\frac{\hbar^2}{2m}\frac{\partial^2}{\partial z^2} + V_0(z) - E_{vac} + \frac{\hbar^2}{2m}(\mathbf{G}_\parallel + \mathbf{k}_\parallel)^2 \right\} \dot{u}_{\mathbf{G}_\parallel}(\mathbf{k}_\parallel, z) = u_{\mathbf{G}_\parallel}(\mathbf{k}_\parallel, z)\ . \tag{126}$$

The resulting basis functions have the form

$$\varphi_{\mathbf{G}_{\parallel}G_{\perp}}(\mathbf{k}_{\parallel},\mathbf{r}) = \left\{a_{\mathbf{G}_{\parallel}G_{\perp}}(\mathbf{k}_{\parallel})u_{\mathbf{G}_{\parallel}}(\mathbf{k}_{\parallel},z) + b_{\mathbf{G}_{\parallel}G_{\perp}}(\mathbf{k}_{\parallel})\dot{u}_{\mathbf{G}_{\parallel}}(\mathbf{k}_{\parallel},z)\right\}\ e^{i(\mathbf{G}_{\parallel}+\mathbf{k}_{\parallel})\mathbf{r}_{\parallel}}\ . \tag{127}$$

The coefficients $a_{\mathbf{G}_{\parallel}G_{\perp}}(\mathbf{k}_{\parallel})$ and $b_{\mathbf{G}_{\parallel}G_{\perp}}(\mathbf{k}_{\parallel})$ are determined in exactly the same way as it is done for the muffin-tins by requiring that the functions are continuous and differentiable at the vacuum boundary. It should be mentioned, that the vacuum basis functions offer less variational freedom than the basis set in the interstitial region does. This can be seen by noting that there are only two functions, $u_{\mathbf{G}_{\parallel}}$ and $\dot{u}_{\mathbf{G}_{\parallel}}$ times the corresponding planar planewave, to be matched to all planewaves of the interstitial region with the same $\mathbf{G}_{\parallel}$. But there are generally far more than two different $G_{\perp}$'s, i.e the number of basis functions in the vacuum region is significantly smaller than in the interstitial region. However, this can be improved rather easily. In Eq. (125) only one energy parameter E_{vac} is used. Instead one can used a whole series of parameters E^i_{vac} to cover an energy region. A possible choice of the energy parameters could be $E^i_{vac} = E^{G_{\perp}}_{vac} = E_{vac} - \frac{\hbar^2}{2m}G^2_{\perp}$, which leads correspondingly to $G_{\perp}$ dependent basis functions $u_{\mathbf{G}_{\parallel}G_{\perp}}(\mathbf{k}_{\parallel},z)$. For more details see Ref. 76. In general, however, the present approximation is accurate, the energy spectrum of the electrons in the vacuum region is small due to the work-function.

Finally we would like to summarize the basis set used for thin film calculation with the FLAPW method:

$$\varphi_{\mathbf{G}_\parallel G_\perp}(\mathbf{k}_\parallel, \mathbf{r}) = \begin{cases} e^{i(\mathbf{G}_\parallel + \mathbf{k}_\parallel)\mathbf{r}_\parallel}\ e^{iG_\perp z} & \text{interstitial} \\ \left\{ a_{\mathbf{G}_\parallel G_\perp}(\mathbf{k}_\parallel) u_{\mathbf{G}_\parallel}(\mathbf{k}_\parallel, z) \right. & \\ \left. + b_{\mathbf{G}_\parallel G_\perp}(\mathbf{k}_\parallel) \dot{u}_{\mathbf{G}_\parallel}(\mathbf{k}_\parallel, z) \right\} e^{i(\mathbf{G}_\parallel + \mathbf{k}_\parallel)\mathbf{r}_\parallel} & \text{vacuum} \\ \sum_L a_L^{\mu \mathbf{G}}(\mathbf{k}) u_l(r) Y_L(\hat{\mathbf{r}}) + b_L^{\mu \mathbf{G}}(\mathbf{k}) \dot{u}_l(r) Y_L(\hat{\mathbf{r}}) & \mathrm{MT}^\mu \ . \end{cases} \tag{128}$$

This expansion has been suggested by H. Krakauer, M. Posternak and A. J. Freeman[31]. Correspondingly, the charge density and potential is expanded in the form:

$$n(\mathbf{r}) = \begin{cases} \sum_s n_s \Phi_s^{3D}(\mathbf{r}) & \mathbf{r} \in \text{interstitial region} \\ \sum_s n_s(z) \Phi_s^{2D}(\mathbf{r}) & \mathbf{r} \in \text{vacuum} \\ \sum_\nu n_\nu^\mu(r) K_\nu(\hat{\mathbf{r}}) & \mathbf{r} \in \mathrm{MT}^\mu \end{cases} \tag{129}$$

and the Hamiltonian and overlap matrix consists now of an additional term (compare to Eq. (55)), the vacuum contribution, paying tribute that the space is now partitioned in three regions

$$\mathrm{H} = \mathrm{H}_I + \mathrm{H}_{MT} + \mathrm{H}_V \qquad \text{and} \qquad \mathrm{S} = \mathrm{S}_I + \mathrm{S}_{MT} + \mathrm{S}_V \, . \tag{130}$$

The Wire Geometry for Chains,Wires and Tubes

In the FLAPW method for one-dimensional systems[46], the infinite three-dimensional space is again partitioned into three regions: the muffin-tin spheres around the atoms, the interstitial region between the atoms and within a cylinder along the axis of the wire (z) of the radius R_{vac}. Outside this cylinder there is an infinitely extended vacuum region (VR in Figure 13). From here on we define the z-axis as the axis of one-dimensional translational symmetry. As our method is based on the use of LAPW basis functions,[19,31,12] the set of reciprocal vectors $\mathbf{G} = (\mathbf{G}_{||}, G_z)$ is generated in a rectangular box, which reflects the translational periodicity of the system in z-direction. The corresponding Bloch number, k_z, lies within the first one-dimensional Brillouin zone. The in-plane reciprocal lattice vectors $\mathbf{G}_{||}$ are generated in an in-plane square lattice with the lattice constant $\tilde{D}$. The vacuum region is an infinite region outside the cylinder with the diameter $D_{\mathrm{vac}} < \tilde{D}$ ($D_{\mathrm{vac}} = 2R_{\mathrm{vac}}$), with the axis along z-direction.

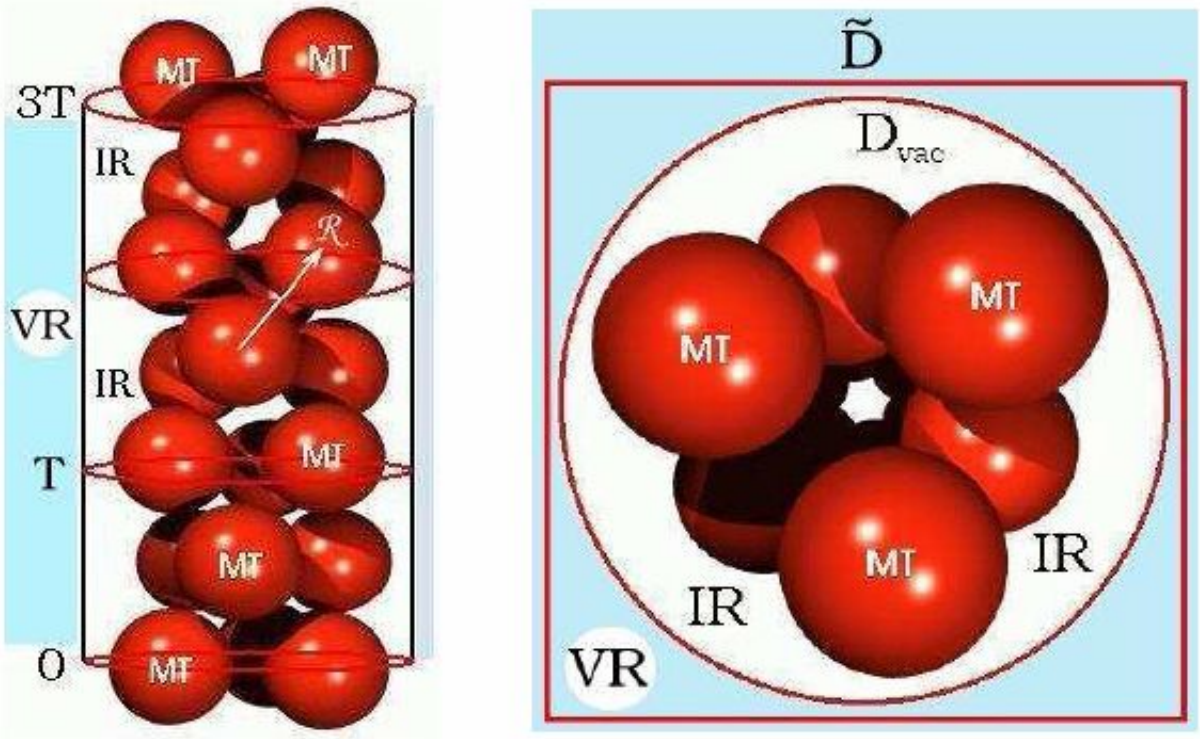

Figure 13. Spatial partitioning of space into muffin-tin spheres (MT), interstitial region (IR) and vacuum region (VR) (shown in blue color) is shown from aside (left) and from the top (right). The vacuum region is the infinite region outside the cylinder with the diameter D_{vac}. In-plane reciprocal vectors $\mathbf{G}_{||}$ are generated in an in-plane square lattice with the lattice constant $\tilde{D} > D_{\text{vac}}$.

As characteristic for the FLAPW method, optimally adjusted basis functions are used it three different regions of space. In the interstitial region and in the spheres, the usual LAPW basis functions are used. In the vacuum the following representation is used:

$$\varphi_{\mathbf{G}}(k_z, \mathbf{r}) = \sum_m \left(a_m^{\mathbf{G}}(k_z)\, u_m^{G_z}(k_z, r) + b_m^{\mathbf{G}}(k_z) \dot{u}_m^{G_z}(k_z, r) \right) e^{im\varphi} e^{i(G_z + k_z)z}. \quad (131)$$

The space coordinate $\mathbf{r}$ is written in terms of cylindrical coordinates (r, φ, z) and the summation over m goes up to the angular expansion parameter $m_{\max}$, which ensures that the oscillations of the plane-waves on the cylindrical vacuum boundary continue smoothly to the vacuum side. Since the vacuum potential is rather flat, relativistic effects on the basis functions can safely be ignored, and the cylindrically symmetrical part of the vacuum potential $V_0(r)$ and the vacuum energy parameter E_v, determined in every iteration, enter in solving the radial Schrödinger equation for every pair (m, G_z) giving rise to the vacuum radial basis wavefunctions $u_m^{G_z}(k_z, r)$ and their energy derivatives $\dot{u}_m^{G_z}(k_z, r)$.

The sets of augmentation coefficients a and b both for the MT spheres and the vacuum region are determined such that the basis functions and their spatial derivatives are continuous across the MT spheres, interstitial and vacuum region boundaries. All the basis functions with reciprocal lattice vector $\mathbf{G}$ that fulfill the condition $|k_z + \mathbf{G}| < K_{\max}$ are included. The corresponding representation of the charge density and potential involves all vectors $\mathbf{G}$ with $|\mathbf{G}| < G_{\max}$. Typically, $G_{\max} \approx 3 \cdot K_{\max}$ in order to describe multiplication of the interstitial potential with the step function. The vacuum parameter $m_{\max}$ is defined in the same manner as $l_{\max}$ in the spheres:[14] $m_{\max} \simeq K_{\max} \cdot R_{\text{vac}}$.